Available online at www.sciencedirect.com
SCIENCE DIRECT®
Journal of Hydrology 279 (2003) 210–223
Journal of Hydrology
www.elsevier.com/locate/jhydrol

Funneled flow mechanisms in layered soil: field investigations

Arik Heilig[a], Tammo S. Steenhuis[a], M. Todd Walter[a,*], Stephen J. Herbert[b]

[a]*Department of Biological and Environmental Engineering, Cornell University, Ithaca, NY 14853-5701, USA*
[b]*Department of Plant and Soil Sciences, University of Massachusetts, Amherst, MA 01003-0910, USA*

Received 21 May 2002; accepted 6 May 2003

Abstract

The movement of water and potential pollutants in the vadose zone of fluvial deposits is often difficult to predict because fine-over-coarse layers may behave as capillary barriers, funneling water and dissolved solutes into concentrated preferential flow paths. Capillary barriers have been studied in laboratory experiments and by mathematical analysis with well-defined boundaries but little is known about water and solute movement in naturally layered soils. This paper demonstrates how naturally occurring capillary barriers affect water and solute movement. Experiments were carried-out in a river valley near Amherst, MA and on a prehistoric beach near Cornell University in Ithaca, NY. Dye tracer and chloride were initially applied near the soil surface, followed by intermittent rainfall over several weeks. After 2–6 weeks the blue dye, soil water content, and chloride concentration distributions in the soil profile were examined by excavating a trench and photographing and sampling the exposed soil face. At both sites, the infiltrating water was diverted and flowed laterally over a relatively coarse layer. At the Cornell site, flow broke through the fine–coarse interface into the coarse layer at a few points along the barrier. The primary breakthrough at the Cornell site occurred at a horizontal section of the interface, 2 m down-slope from the point of dye application. The capillary diversions generally agreed with current theory, however, the flow patterns were difficult to predict accurately without more detailed information about the soil layering characteristics.

Keywords: Capillary barrier; Vadose zone; Unsaturated flow; Diversion flow; Breakthrough flow

1. Introduction

Capillary barriers are currently of acute interest because of their potential to funnel water away from sensitive underground regions (Selker, 1997; Webb, 1997; Morris and Stormont, 1997). They also affect the movement and distribution of land-applied chemicals in a natural setting and potentially increase the danger of groundwater contamination by decreasing the travel time and contact area. In situ capillary barriers most commonly occur naturally in fluvial deposits and in seashore soils (Kung, 1990a; Boll et al., 1996).

Capillary barriers occur at sloping interfaces between texturally distinct soils with fine soil overlaying a coarser soil layer. The unique flow around these barriers is commonly referred to as *funneled flow* (Kung, 1990b, 1993). For a continuous fine–coarse interface, three distinct, steady state funnel flow regimes can be generalized (Walter et al., 2000):

* Corresponding author. Tel.: +1-607-255-2488; fax: +1-607-255-4080.
E-mail address: mtw5@cornell.edu (M.T. Walter).

0022-1694/03/$ - see front matter © 2003 Elsevier B.V. All rights reserved.
doi:10.1016/S0022-1694(03)00179-3

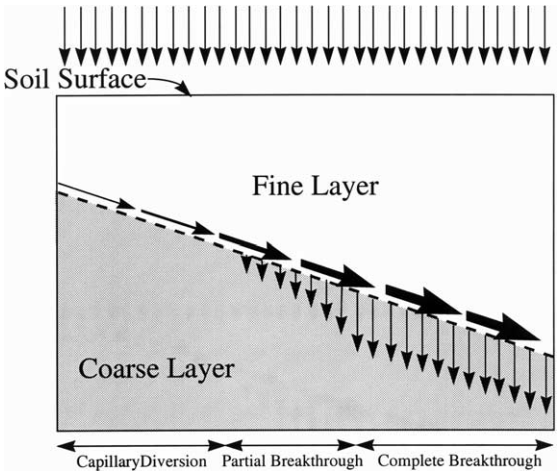

Fig. 1. A schematic presentation of the diversion of water over a textural discontinuity that acts as a capillary barrier. Arrows indicate water flow.

the capillary diversion, the partial breakthrough, and a complete breakthrough (Fig. 1). The term capillary diversion refers to the process in which percolating water is diverted laterally over a coarse soil layer. This occurs where the unsaturated hydraulic conductivity of the fine soil is higher than the coarse layer below (Miyazaki, 1988; Ross, 1990). The length of the diversion depends largely on the flow rate and the slope of the fine–coarse interface (Walter et al., 2000). Water accumulates down-slope in the capillary diversion zone necessarily resulting in decreasing matric potential and correspondingly increasing hydraulic conductivity. If the textual interface is long enough and flow is continuous, at some point along the interface the matric potential will be high enough that water will penetrate into the underlying coarse layer. This is the initiation of breakthrough. The region where the vertical flux into the coarse layer is less than the water application rate is the partial breakthrough zone. In the last decade researchers have claimed that *breakthrough* will not occur until the matric potential in the fine layer is at or above the water entry value derived from the wetting branch of the soil water characteristic curve of the coarse soil (Rasmuson and Erikson, 1988; Kung, 1990b; Ross, 1990; Steenhuis et al., 1990). However, recent research has shown that breakthrough may develop before this water entry value is reached (Walter et al., 2000). Full breakthrough occurs where the vertical flux penetrating the coarse layer equals the water application rate and, thus, the net lateral flow is constant in the full or complete breakthrough region (Fig. 1).

The maximum length of the capillary diversion zone was quantified by Ross (1990) and Steenhuis et al. (1991) assuming an infinite interface and that water enters the coarse layer at the water entry value, ψ_w^*. The maximum diversion length, L, under steady state conditions can be expressed as

$$L = \tan(\beta)\frac{K_s}{q}\left[\frac{1}{\alpha} + (|\psi_a| - |\psi_w^*|)\right] \quad (1)$$

where $\tan(\beta)$ is the slope of the interface, K_s is the saturated hydraulic conductivity of the fine layer, q is the infiltration rate, ψ_a is the air entry value into the fine layer, and α is a characteristic exponent describing hydraulic conductivity (Gardner, 1958; Ritsema et al., 1996). The hydraulic conductivity for the fine layer can be expressed as

$$K = K_s \exp(\alpha\psi) \qquad \psi \le \psi_a \quad (2a)$$

$$K = K_s \qquad \psi > \psi_a \quad (2b)$$

where ψ is the matric potential. Predictions using these equations were compared with laboratory measurements and agreed well when ψ_w^* was replaced by the matric potential at which initial breakthrough into the coarse layer occurred (Walter et al., 2000).

This study focuses on the flow over and through capillary barriers that occur naturally in the environment. In spite of their prevalence, very few studies have examined the flow pattern of water and solutes around these natural features. In the central sand area of Wisconsin, Kung (1990a) applied red dye (Rhodamine WT) in the spring-time and, upon excavation in the fall, found the dye concentrated along an inclined textural interface 1.5 m below the surface. Very little dye was recovered from below the interface. This study continues in the same vein as Kung (1990a) to help further our understanding of the effects of layering in soils on water and solute movement. The main objective of this study is to detail the effects of in situ capillary barriers on water and solute movement at two field sites and to explore application of a model to these conditions.

2. Material and methods

Field experiments were conducted on two different sites with distinctive, sloping soil layers. The first site was located 200 m west of the Connecticut River on the University of Massachusetts' experimental farm near Amherst, MA. The experiment commenced on June 19, 1997 and ended on July 21, 1997. The second site was located near the Cornell University campus in Ithaca, NY. This site was the shore of a prehistoric sea. Experiments at Cornell ran from August 12, 1997 to September 25, 1997. At both locations, the soil surface was nearly level, less than a 1% slope.

The experimental process was: (1) initially place blue dye (FD&C blue dye #1) sources near the soil surface and apply chloride (Cl) uniformly over the site, (2) irrigate weekly for several weeks, and (3) excavate the site to examine water and chemical distributions throughout the soil profile. The powdered blue dye was buried 20 cm deep, just below the root zone. Chloride was applied as $CaCl_2{\cdot}6H_2O$ salt on the study site surface at 75 g Cl m^{-2}. The areas of Cl application were 0.5×3 m^2 at Amherst and 2×3 m^2 at Cornell. Each site was irrigated approximately 12–13 h, once a week with 2 overlapping mini Rainbird sprinklers at a rate of 7.5 mm h^{-1}. To facilitate sampling, several weeks after the experiment commenced a vertical soil face was exposed by excavating a trench adjacent to the experimental area. The blue dye distribution was photographed. Chloride concentration and water contents were obtained by taking closely spaced soil samples across the exposed soil face. The water content of each sample was measured by oven drying at 105 °C. The Cl concentration was measured using a digital Buchler chloridometer. Soil particle size distribution was determined on a subset of these samples using mechanical sieving, to separate the sand particles larger than 250 μm, and a hydrometer to determine the small sand (<250 μm), silt and clay percentages. Unique aspects of the two sites are discussed below.

At the Amherst site, 45 cm of water was irrigated on four occasions, June 26, July 3, July 10, and July 17. In addition, 9.5 cm of rain fell during the experiment. Blue dye was applied as two point sources. The dye distribution was observed and soil samples were taken using Ritsema et al. (1996) methodology on July 21, one day after the last rainfall. Twenty cylinders (5 cm diameter and 10 cm height) were inserted into the soil side by side in a horizontal row and each sample was put in a plastic bag. This process was repeated in 10 cm depth increments to a depth of 110 cm (11 rows and 20 samples per row). The samples were tested for water content and Cl concentrations as described above.

At the Cornell site, blue dye was applied as line sources to facilitate multiple excavations throughout the experiment; excavation trenches ran perpendicular to the line sources. One line of dye was applied at the beginning of the experiment and another after the site had received 22 cm of water (irrigation and natural rainfall). An observation trench was excavated after 22 cm of water had been applied and the exposed face was re-excavated twice more after cumulatively applying 64 and 75 cm of water, respectively. After the last excavation, which was one and a half days after the last irrigation, 350 soil samples were collected using methods similar to the Amherst experiment. Because of the size and complexity of some portions of the profile, some samples were taken by hand instead of using the sampling cylinders. Samples were tested for water content and Cl using the techniques discussed above.

Because, as will be discussed in Section 3, the Amherst site had a relatively well-defined soil profile, a comparison was made between diversion lengths predicted with the previously discussed simple capillary barrier model (Eq. (1)) and the observed diversion. To parameterize the model for the Amherst site, the saturated conductivity and the drying branch of the water retention curve were measured for the different soil layers. The saturated hydraulic conductivity was measured using the constant head method (Klute et al., 1965) and the drying branch of the water retention curve was measured using the hanging water method (Veneman, 1974). To estimate the Gardner α parameter used in Eqs. (1) and (2a), the following procedure was used: (i) the van Genuchten water retention function (van Genuchten, 1980) was fit to the measured water retention data to estimate the characterizing van Genuchten parameters, (ii) the measured hydraulic conductivity curve was estimated using these parameters (van Genuchten, 1980), and (iii) the α in the Gardner type hydraulic conductivity was estimated by fitting Eq. (2a) to the van Genuchten relative hydraulic conductivity.

Table 1
Soil characteristics at Amherst, MA

Soil layer	Clay (%)	Silt (%)	Sand < 250 μm (%)	Sand > 250 μm (%)	Texture
Plow	4.3 (0.5)	10.6 (1.1)	60.2 (2.1)	24.9 (1.5)	Loamy sand
Fine sand	5.2 (0.6)	7.7 (0.7)	58.5 (1.3)	28.6 (1.1)	Sand
Coarse sand	3.1 (0.1)	0.7 (0.05)	39.1 (1.2)	57.1 (1.8)	Sand

Numbers in ( ) are standard deviations.

3. Soil profiles at each site

3.1. The Amherst site

Based on texture analysis, the cross-section was divided into three regions (Table 1): *Plow Layer*, *Fine Sand* and *Coarse Sand* (Fig. 2). The *Plow Layer* is classified as loamy sand, and although both the *Fine* and the *Coarse Sands* are classified as sand, the *Fine Sand* has particles predominantly smaller than 250 μm, and in the *Coarse Sand* they are larger than 250 μm. The dashed line in Fig. 2 shows the general location of the interface between the *Fine* and the *Coarse Sands*. The average interface depth is 85 cm with a slope of 8% downward from left to right (Fig. 2). Fig. 3(a)–(c) show the water retention curves and the hydraulic conductivity functions for the *Fine* and the *Coarse Sands*. The specific soil hydraulic properties, Gardner's α, and van Genuchten parameters are shown in Table 2. The Gardner's α agreed well with the range of values published by Khaleel and Relyea (2001) for sandy soil; their lowest, 0.0013 cm^{-1}, was lower than our *Fine Sand* α, 0.02 cm^{-1}, and their highest, 0.13 cm^{-1}, was slightly higher than our *Coarse Sand* α, 0.11 cm^{-1}. To further check our conductivity curves we used published parameters for the Campbell (1974) $K(\theta)$ function; the error bars in Fig. 3(b) and (c) correspond to the range of curves obtained in this way. For *Fine Sand*, published Campbell parameters generally ranged between 3 and 5 (e.g. Topp, 1969; Haridasan and Jensen, 1972; Bhatnagar et al., 1979; Sisson and vanGenuchten, 1992) and for *Coarse Sand* between 0.5 and 4 (e.g. Vachaud, 1967; Staple, 1969; Gupta et al., 1977; van Genuchten and Nielsen, 1985). Fitting the Gardner equation to the outer boundaries depicted by the error bars in Fig. 3(b) and (c) provided a range of Gardner α for each sand, i.e. for *Fine Sand* $\alpha = 0.015–0.025$ cm^{-1}, and for *Coarse Sand* $\alpha = 0.08–0.15$ cm^{-1}, which corroborated our experimental values and can be used to assess the uncertainty in our calculated funnel flow diversion lengths.

3.2. The Cornell site

The textural composition of the Cornell site was much more complicated than the Amherst site. The cross-section was divided into five layers shown in Fig. 4 and Table 2. The *Top* layer was relatively uniform loamy sand. The *Micro-Layered* region, lying below the *Top* layer, was, on average, about 30 cm wide and dips from left to right in the figures. The *Micro-Layered* region was a matrix of closely spaced

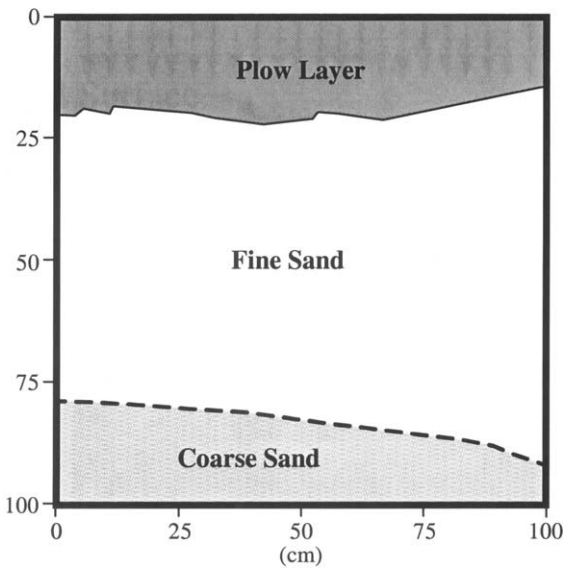

Fig. 2. Schematic of the soil profile at Amherst.

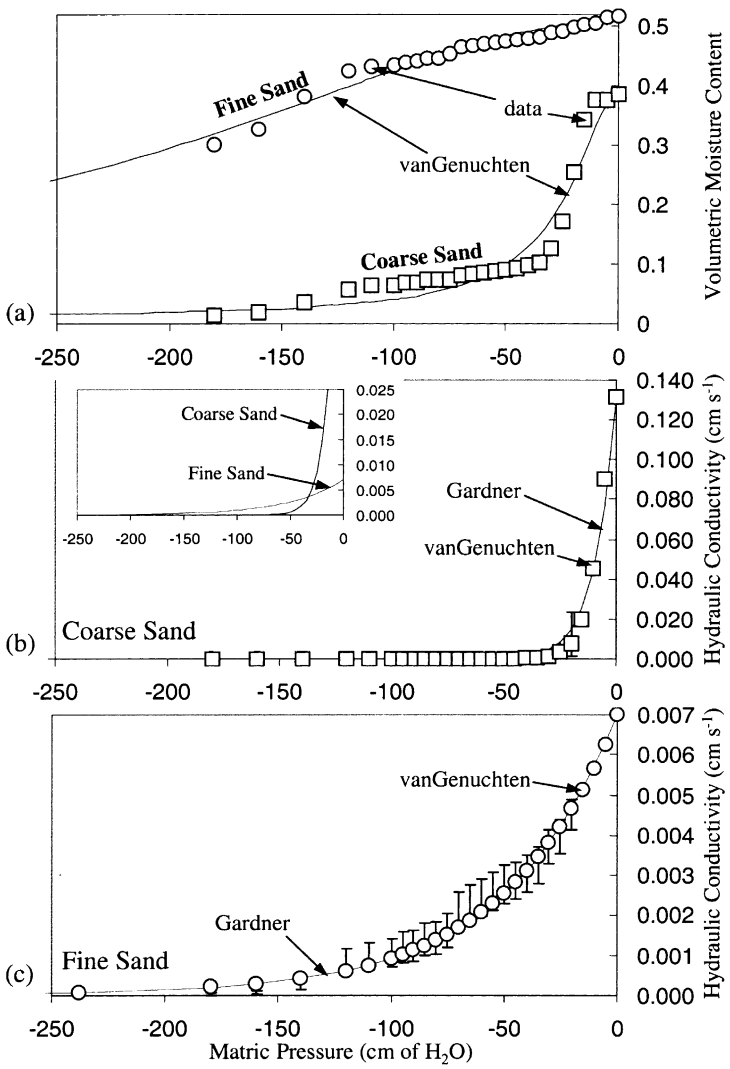

Fig. 3. Soil characteristics at Amherst: (a) drying water retention curves for the *Fine* and the *Coarse* layers, data are shown as symbols and the lines are the fitted van Genuchten curve; (b) and (c) are the hydraulic conductivity functions of the *Coarse* and *Fine* layers, respectively, symbols are van Genuchten curves and the lines are the fitted Gardner curves (Eq. (2)). The error bars are from published Campbell (1974) relationships for similar soil types. The inset shows the hydraulic conductivities for both soils superimposed on one another.

fine and coarse sands of non-uniform widths; some are narrower than 1.0 cm and some as wide as 5 cm. The bottom part of the *Micro-Layered* region was predominantly sand particles that are smaller than 250 μm. A *Sandy Loam* pocket was located between the *Top* layer and *Micro-Layered* regions on the right side of the profile (Fig. 4). Below the *Micro-Layered* region was the *Coarse Sand* layer that varied from 15 to 2.5 cm thick and was predominantly comprised of

Table 2
Soil hydraulic characteristics at Amherst, MA

Soil layer	θ_s (cm^3 cm^{-3})	K_s (cm s^{-1})	Gardner α (cm^{-1})	vanGenuchten	
				α	n
Fine sand	0.51	0.0070	0.02	0.0074	1.89
Coarse sand	0.39	0.13	0.11	0.056	2.38

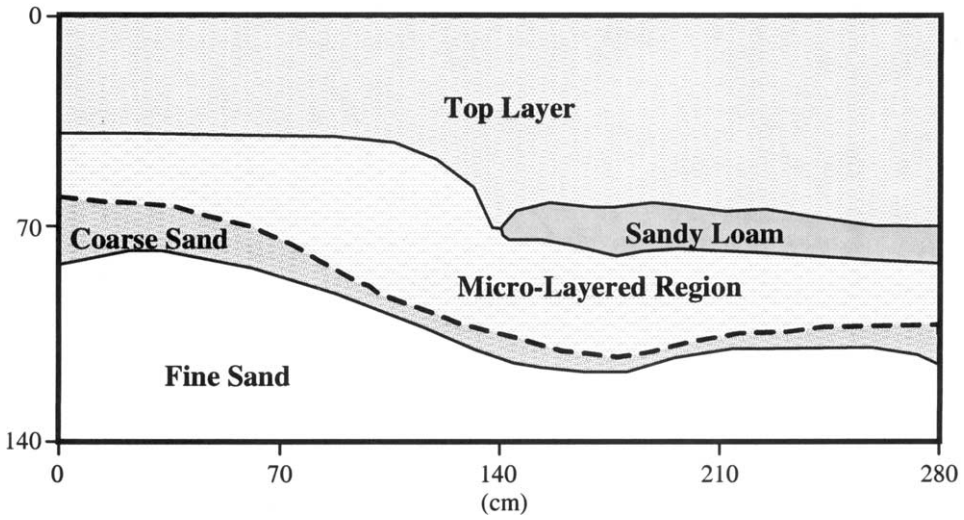

Fig. 4. Schematic of the soil profile at Cornell.

sand particles larger than 250 μm. The boundary between the *Micro-Layered* region and the *Coarse Sand* was shown with a dashed line in Fig. 4. The geometry of this interface was more complicated than the fine–coarse boundary at Amherst. The interface was relatively horizontal on the left-hand side of Fig. 4, it dipped steeply (30% slope) to the right between horizontal distances 20 and 175 cm, was relatively level around 180 cm, and then sloped up to the right at about 8% beyond 190 cm. As expected, and as will be shown later, the geometry of this interface affected the flow pattern of the water, dye, and Cl. Under the *Coarse Sand* was the *Fine Sand*, dominated by particles smaller than 250 μm. Because of the micro-layering at the Cornell site, the soil water characteristic curve obtained from above the main interface was not meaningful.

4. Results and discussion

4.1. The Amherst site

The dye distribution in the Amherst experiment after 55.0 cm of infiltrated water is shown in Fig. 5. Arrows indicate the buried dye locations and the dashed line shows the fine and coarse sand interface. The dye clearly moved at least 1 m laterally over the *Coarse Sand*. Occurrences of breakthrough were not obvious from the dye, however, faint dye patterns around 0 (very faint) and 35 (most noticeable), appeared to be due to isolated breakthroughs, probably during isolated periods of high water application. Note that some dying below the interface occurred when dyed soil fell down while we were cleaning the 'soil face', (10–30 cm). Despite these isolated occurrences of possible breakthrough, Fig. 5 shows relatively strong evidence of lateral flow diversion by the capillary barrier at the fine–coarse interface. The characteristics of the soil profile's water distribution and Cl concentrations are discussed in more detail below.

Fig. 6 shows that the volumetric water content near the soil surface generally is the highest and then decreases gradually with depth in the *Fine Sand*. As with the dye, the water distribution shows clear evidence of a capillary barrier at the fine–coarse interface. There is a sharp decrease in water content going from the *Fine Sand*, 0.18–0.25 $cm^3\ cm^{-3}$, to the *Coarse Sand*, 0.05 $cm^3\ cm^{-3}$ (Figs. 6 and 7). Fig. 6 shows evidence of partial breakthrough at horizontal distances 0, 38, and 55 cm as indicated by isolated dips or lobes of relatively high water content penetrating the interface. The dye results, although much less obvious, corroborated the 0 and ~38 cm locations. The relatively low water contents at 0, 35, and 55 cm at 10 cm above the interface in the *Fine Sand* (Fig. 7) correspond to these lobes. This is

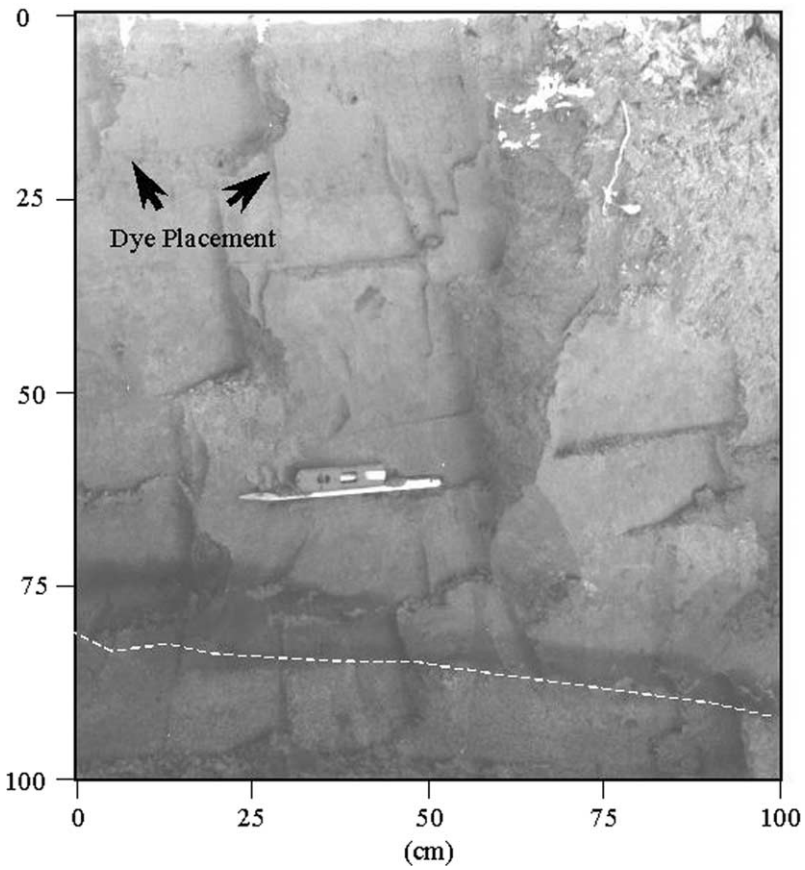

Fig. 5. The volumetric water content distribution in the soil profile at Amherst; the dark color is wettest and the light is driest. The dashed line shows the fine–coarse interface. The white arrow shows approximate flow direction.

consistent with Cho et al. (1999), who found that the water content above the point of finger initiation is lower than the surrounding soil. The *Coarse Sand* water contents 10 cm below the interface (Fig. 7), do not show evidence of breakthrough indicating that the breakthrough of water was relatively minor. Breakthrough flow will be discussed in more detail later. Finally, the water content measurements in Fig. 7 show clearly that the *Fine Sand* is wetter on the right-hand and down-slope side than on the left-hand and up-slope side of the profile (Fig. 7). This trend is in agreement with capillary diversion flow, namely, the water content is higher down-slope above the capillary barrier due an accumulation of laterally diverted water over the barrier. The soil below the barrier remains dry. Interestingly, there is a relatively high water content region at about 50 cm depth that extends laterally between 25 and 100 cm. It is not obvious why this relatively high water content region is located here nor how it affected the observed patterns at this site.

The Cl distribution in the profile, shown in Fig. 8, also provides some insights into the flow around the fine–coarse interface. Assuming our sample surface characterizes the entire width of the Cl application area, i.e. perpendicular to the sample surface, only 9.7% of the applied Cl was accounted for in the sampled region, and thus it is probable that most of the Cl leached out before sampling. Some Cl loss may also be due to lateral dispersion at the edges of the study area. As with the dye, the Cl is relatively concentrated above the fine–coarse interface suggesting a capillary barrier restricted vertical water movement into the *Coarse Sand*. As with

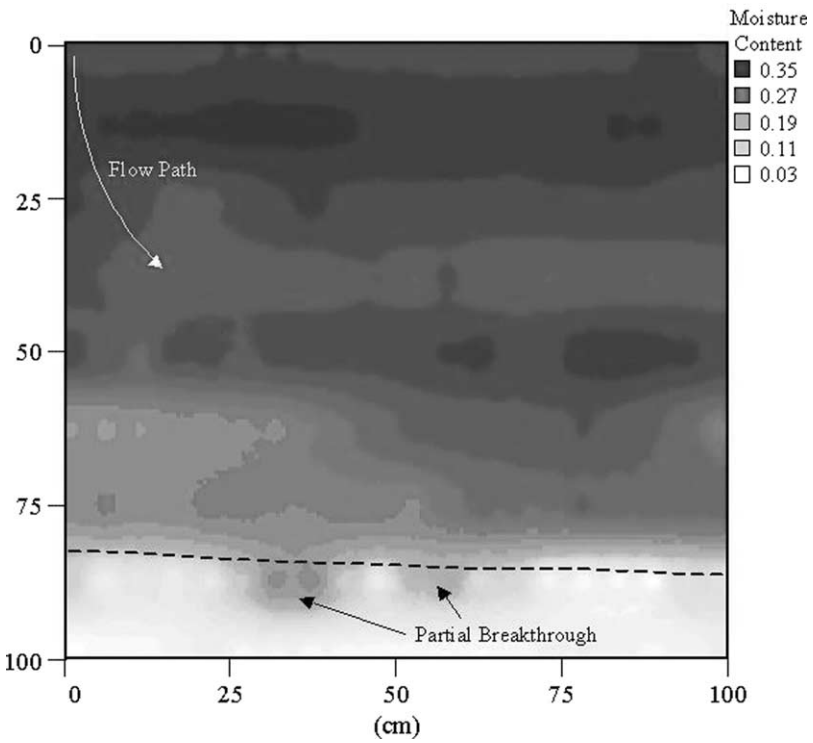

Fig. 6. The volumetric water content distribution in the soil profile at Amherst. The dashed line shows the fine–coarse interface.

the dye distribution in Fig. 5 and water concentrations in Fig. 6, the Cl concentrations in Fig. 8 suggest a few isolated locations of limited breakthrough, most notably at horizontal distances 0 and 45 cm. There is no evidence that Cl, or water, penetrated the barrier to any significant depth, thus most of the Cl was probably leached out to the right side of the sampled profile. The dye showed less evidence than the Cl of leaching because it is slightly sorbed to the soil. The dye and the Cl distributions in Figs. 5 and 8 do not support a breakthrough at 55 cm as was indicated by the water content (Fig. 6). The curiously high Cl concentration in Fig. 8 on the left-hand side or up-slope region relative to the right-hand side or

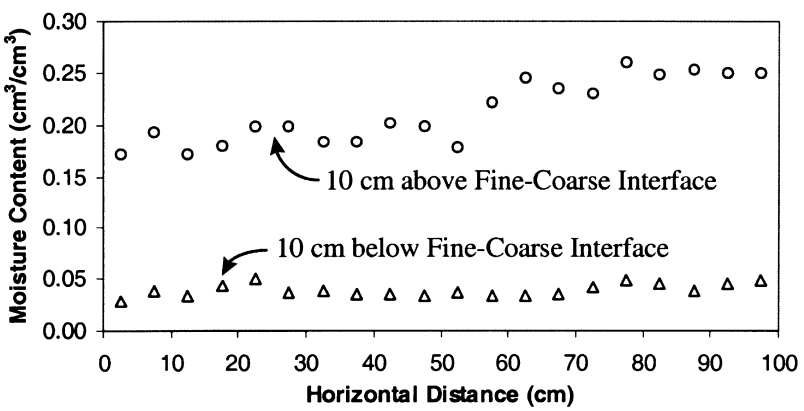

Fig. 7. The water content at Amherst at sampling points 10 cm above and 10 cm below the fine–coarse interface.

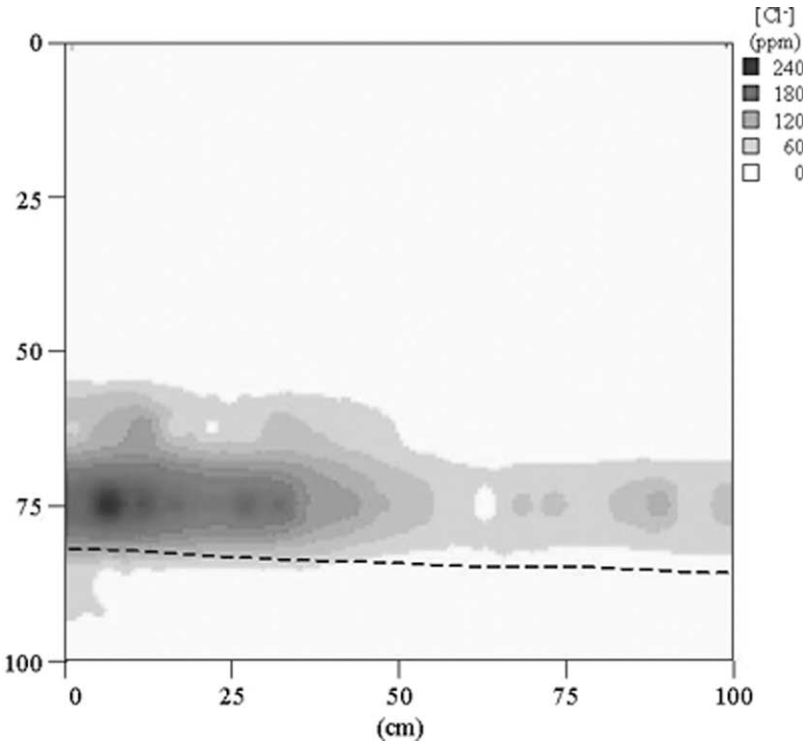

Fig. 8. The chloride distribution in the soil profile at Amherst. The dark color indicates high concentration. The dashed line shows the fine–coarse interface.

down-slope region seems initially counterintuitive but matches the dye distribution very well (Fig. 5). The high up-slope Cl concentration is also consistent with the other findings when we take into account that most of the Cl probably had already leached from the profile. As discussed in the paragraph above, most lateral flow is occurring at the right-hand (down-slope) side and the smallest amount on the left-hand side. We expect, therefore, in accordance with the results in Fig. 8 that in the higher flux areas more Cl is leached out than in the low flux areas. We acknowledge that our discussion and interpretations assume two-dimensional flow and some patterns and results (e.g. Cl recovery), may have explanations that need to include the third dimension for which we have no additional information to aid our analysis.

It is of interest to examine if current funnel flow theory can be used to corroborate the observed diversion. To do this, Eq. (1) was employed. The matric potential in the *Fine Sand* and the associated hydraulic conductivity of the *Coarse Sand* were estimated from the water content near the interface. One day after the last rain, the highest measured water content above the fine–coarse interface was 0.25 $cm^3\ cm^{-3}$ (Fig. 7). The matric potential associated with this water content is −280 cm (Fig. 3(a)). At a matric potential of −280 cm, the associated hydraulic conductivity of the *Coarse Sand* is 1.7×10^{-8} cm s^{-1}, which is much less than the hydraulic conductivity in the *Fine Sand*, 1.2×10^{-4} cm s^{-1}. During irrigation, the matric potential in the *Fine Sand* was probably higher and it is likely that during short periods water could flow across the boundary explaining the limited breakthrough observed in Figs. 5, 6, and 8. In order to test Eq. (1), the air entry value of the *Fine Sand* and water entry value of the *Coarse Sand* need to be estimated. Both curves shown in Fig. 3(a) are drying curves and the air entry values are uncertain; a very conservative assumption is, that the water entry value of the *Coarse Sand* is the same as the air entry value of the *Fine Sand*. To calculate the maximum breakthrough length

Table 3
Soil characteristics at Cornell

Profile region	Clay (%)	Silt (%)	Sand < 250 μm (%)	Sand > 250 μm (%)	Texture
Top layer	2.9 (0.6)	11.5 (3.6)	61.5 (4.3)	24.1 (3.3)	Loamy sand
Sandy loam	8.5 (0.3)	13.7 (1.0)	0.0 (–)	77.7 (1.1)	Sandy loam
Micro-layered	4.0 (0.8)	6.5 (0.7)	52.3 (3.7)	37.2 (0.3)	Sand
Coarse sand	2.7 (0.2)	4.4 (0.7)	33.5 (2.5)	59.4 (0.8)	Sand
Fine sand	3.6 (0.3)	17.6 (2.6)	48.8 (2.5)	30.0 (2.3)	Sand

Numbers in ( ) are standard deviations.

the infiltration rate was taken as the irrigation rate of 0.18 m day^{-1} and the interface slope, tan(β) is 8%. From Table 3, the *Fine Sand* $\alpha = 0.02\ cm^{-1}$, but values between 0.015 and 0.025 cm^{-1} represent the uncertainty in our estimate of α. The saturated conductivity of the *Fine Sand* is 0.007 cm s^{-1}. Using these parameters, the predicted maximum diversion length using Eq. (1) is between 1.08 and 1.79 m. The observed diversion length at the Amherst site was at least 1 m, which is just below the range of maximum diversion length predicted from Eq. (1). Although, the overall diversion is explained by Eq. (1), the minor breakthrough at the upper end is not. It is probable that small inconsistencies along the interface play important roles in promoting breakthrough and current applications of the theory do not account for these.

4.2. The Cornell site

Fig. 9(a)–(c) shows the dye distributions in the profile after 22, 64, and 75 cm of water application, respectively. The boundaries between important soil layers shift slightly because each picture is of a slightly different profile. The arrows in Fig. 9(b) show the locations of dye application. It is evident from these figures that water moved laterally in the *Micro-Layered Region* and that the flow was considerably more complicated than at Amherst. The inserts in Fig. 9(a) show some of the micro-complexity within the *Micro-Layered* soil along the interface separating the *Micro-Layered* and the *Coarse Sand* soils. Although the particle size distribution was not dissimilar to the Amherst site, both the small thickness of the *Coarse Soil* and the complicated layer geometry are significant factors influencing the flow pattern in the Cornell site and therefore, unlike at the Amherst site, Eq. (1)'s applicability was limited. How layer geometry affected the flow pattern is discussed below. Note that as with the Amherst site, the third dimension probably influenced results but, due to insufficient information in this dimension, we have omitted this aspect from our discussion.

After 22 cm of water application, the observed lateral diversion within the *Micro-Layered* region was 130 cm (Fig. 9(a)). The dye concentrated in the area marked 'i' (Fig. 9(a)) suggests diversions along micro-fine–coarse interfaces within the *Micro-Layered* region, i.e. along interfaces other than the prominent boundary between the *Micro-Layered* and *Coarse Sand* soils (shown as a dashed line in the figures). Closer examination in the field showed also many small sequences of fine–coarse soil. The water was diverted down-slope over these micro-coarser layers and then either penetrated through at some point or percolated downward at the end of a micro-layer (see detail of area 'i'). This was a special case of funneled flow and termed 'Cascade Flow'. The largest lateral diversion of water and dye occurred along the prominent interface separating *Micro-Layered* and *Coarse Sand* soils. Close-ups are given for the areas indicated by 'ii' and 'iii' in Fig. 9. In area 'iv', where the interface was relatively horizontal, the dye moved vertically downwards, penetrating into the *Coarse Sand* layer. The breakthrough at 'iv' was well explained by Eq. (1); i.e. the slope, tan(β), was zero, therefore, the lateral diversion was zero. Note that the vertical, breakthrough distance in area 'iv' was much shorter than the lateral diversion distance along the interface suggesting that the amount of percolating water was much smaller than the amount of water moving laterally. In fact, the lateral flow reached a greater depth, as seen at 'iii', than the vertical movement at 'iv'.

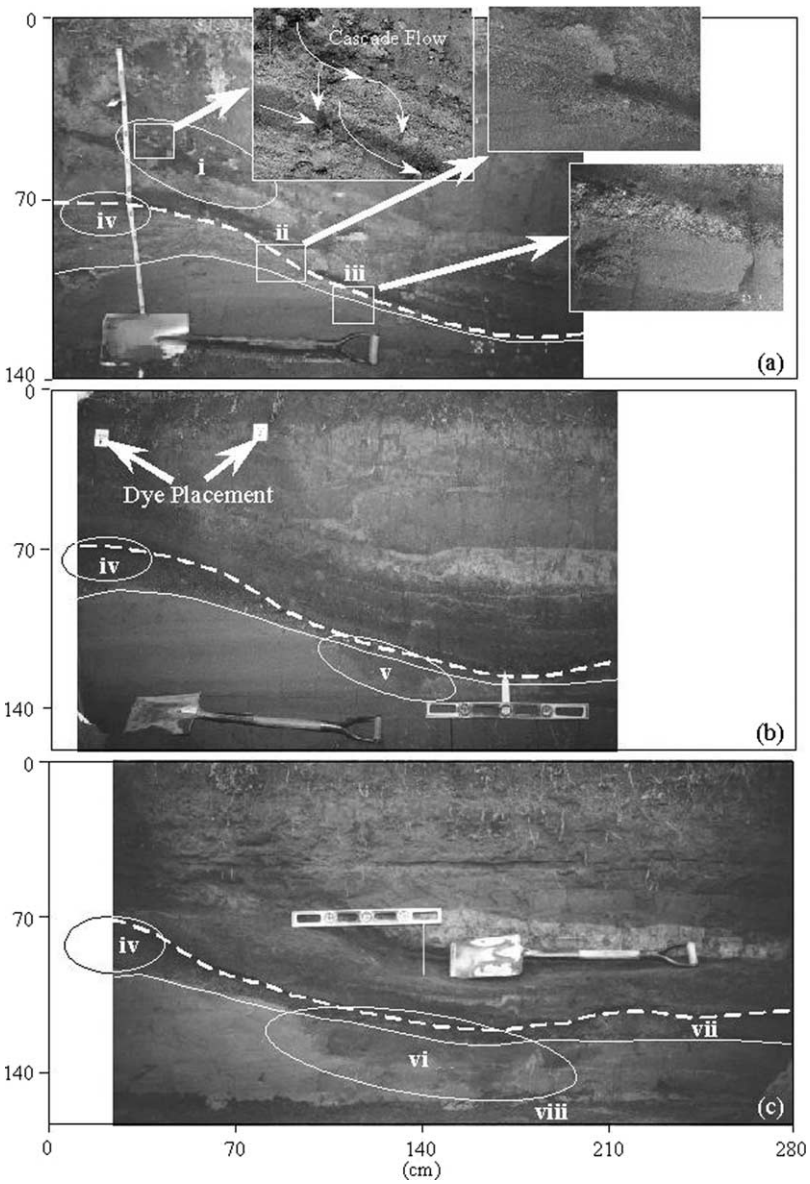

Fig. 9. Photos of the dye distribution at Cornell after the plot received (a) 22 cm of water; (b) 64 cm of water and (c) 75 cm of water. The dashed line shows the interface between the *Micro-Layered* and *Coarse Sand* soils and the solid line the interface between the *Coarse Sand* and the *Fine Sand*.

Fig. 9(b) gives the dye distribution after 64 cm of applied water and the addition of the second line source of dye. The second dye source shows similar 'Cascade Flow' in the *Micro-Layered* region as in Fig. 9(a). Breakthrough penetrating the interface separating *Micro-Layered* and *Coarse Sand* soils was observed now at the area marked 'v'; this area overlaps the area marked 'iii' in Fig. 9(a) and it is not clear why no breakthrough occurred earlier. The breakthrough zone in area 'iv' expanded very little from Fig. 9(a) and is consistent with earlier theoretical findings. Once the water moved through the coarse layer to the fine layer below 'v', the matric potential lowered sufficiently that water flowed to this

breakthrough point, stopping the downward flow at 'iv'. Note that the breakthrough at 'iv' never fully penetrated the coarse sand layer. This is similar to the fingering phenomena (Selker et al., 1992; Liu et al., 1994; Cho et al., 1999) in which one finger will grow sufficiently to stop the development of neighboring fingers due to a lowering of the matric potential in the distribution zone, similar to the capillary fringe here.

This hypothesis of larger flow through area 'v' is supported by Fig. 9(c), which shows the dye distribution after 75 cm of water was applied. The breakthrough zone at 'v' in Fig. 9(b) expanded to area 'vi' in Fig. 9(c). As expected, additional dye penetrating into the *Coarse Sand* appears to have moved freely and directly into the *Fine Sand* below (Fig. 9(b) and (c)).

Fig. 10 shows the water distribution throughout the profile at the Cornell site one and a half days after the last water application. As opposed to the uniformly low water content below the interface at Amherst, the water content in the *Coarse Sand* layer increases to the right along the slope as expected with breakthrough. Fig. 10 also confirms that the breakthrough at area 'iv' has stopped as evidenced by the generally low water contents in the *Fine Sand* below area 'iv'. In Fig. 10 there are relatively high water contents in the *Fine Sand* below the major breakthrough points indicated by areas 'v' in Fig. 9(b) and 'vi' in Fig. 9(c). Although these relatively high water contents corroborate the breakthrough points, they may also indicate textural differences, i.e. the *Fine Sand* has a relatively high water holding capacity. Thus, moisture distributions, i.e. static data, are not always good indicators of flow phenomena alone, especially in complex profiles like this one. Curiously, there is also high water content below area 'vii' (Figs. 9c and 10) and low water content above it; this is consistent with the textural implications, i.e. finer soils generally have higher moisture holding capacities than the coarser soils. Based on the lack of dye in this region (Fig. 9(c)) it seems only limited amounts of water flowed through the interface in region 'vii'. The water in 'vii' may have come from the main breakthrough area 'v'/'vi' and flowed around a possibly coarser area 'viii' imbedded in the *Fine Sand* (Figs. 9(c) and 10). However, based on the water contents alone, a major breakthrough at 'vii' cannot be ruled out; it is possible that the dye does not reach this region because of the dye's absorptive properties. Finally, the right-hand side of the profile in both the *Micro-Layered* and the *Coarse Sand* regions are wetter then the left-hand sides, indicating an accumulation of water due to lateral flow.

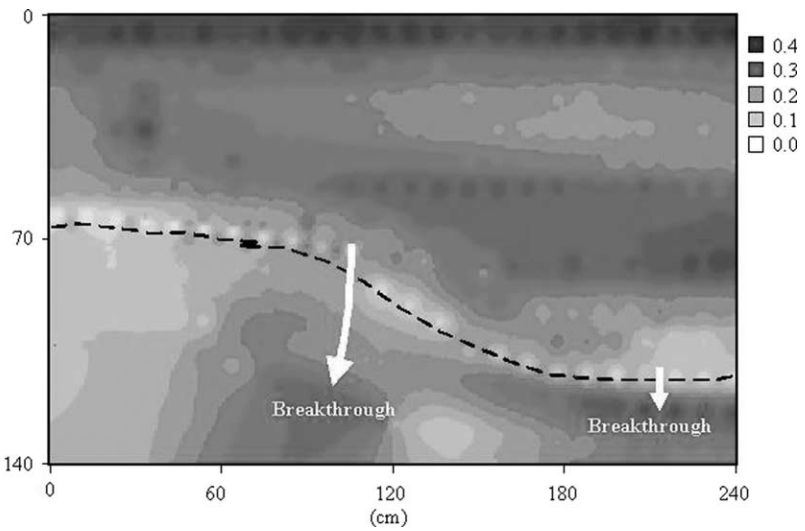

Fig. 10. The volumetric water content distribution in the soil profile at Cornell after 75 cm of water. The dark color is wettest and the light is driest. The dashed line shows the interface between the *Micro-Layered* and the *Coarse Sand* soils.

Because only a small fraction of the Cl was reclaimed in sampling at the Cornell site (5.2%), explanations for the data distribution were inconclusive (data not shown).

The soil profiles of these study sites were representative of places where sediments have been sorted by rivers or coastal processes. These results, combined with the pervasiveness of areas with similar geology and geomorphology, illustrate the widespread prevalence of capillary barriers in the natural environment and the complexity they introduce into predicting the movement of water and chemicals in the vadose zone. While the general theories about funneled flow (e.g. Kung, 1990b; Ross, 1990) are actualized in our data, it is difficult to meaningfully apply mechanistic models, like Eq. (1), to situations where the textural layering is complicated, as at the Cornell site in this study. As with the reasonably good, modeled diversion length results for the Amherst site, it may be possible to successfully apply capillary diversion models to situations where textural layers are discrete, relatively thick, and spatially extensive. It is likely that in complex layered soils, like the Cornell site, the phenomena will need to be investigated at different scales than those previously used in order to determine how to incorporate funnel flow into predictive models. Both smaller and larger scales may provide valuable information.

5. Conclusions

Natural capillary barriers consisting of a relatively fine layer above coarser material were studied. Substantial impacts of these types of textural discontinuity on the movement of water and solutes were observed at two sites in the northeastern United States. Observations of dye, water, and Cl at the Amherst site demonstrated a capillary diversion with possible limited breakthrough for the sampled area. An estimate of the maximum diversion length using a simple, theoretical equation supported the observed diversion. The flow pattern at the Cornell site was considerably more complex than at the Amherst site. Breakthrough occurred first at the flat portion up-slope region but then shifted to a more down-slope location after more water was applied. These field observations generally corroborated previous laboratory and model results. However, it is clearly difficult to predict flow patterns in some naturally layered soils without detailed information about the soil. Even after excavating the soil profile it was difficult to obtain information needed to predict accurately the entire flow pattern observed at the Cornell site using currently derived methods.

Acknowledgements

This research was supported in part by Postdoctoral Award No. FI-230-96 from **BARD**, The United States—Israel Binational Agricultural Research and Development Fund and the USDA. The authors wish to thank Jay Daliparthy for his valuable assistance on this project. We would like to thank Dr G. Clarke Topp for his insightful and cogent comments and suggestions.

References

Bhatnagar, D.Y., Nagarajarao, Y., Gupta, R.P., 1979. Influence of water content and soil properties on unsaturated hydraulic conductivity of some red and black soils. Z. Pflanzenernähr. Bodenk. 142, 99–108.

Boll, J., Van-Rijn, R.P.G., Weiler, K.W., Ewen, J.A., Daliparthy, J., Herbert, S.J., Steenhuis, T.S., 1996. Using ground penetrating radar to detect layers in a sandy field soil. Geoderma 70 (2–4), 117–132.

Campbell, C.S., 1974. A simple method for determining unsaturated conductivity from soil moisture retention data. Soil Sci. 117, 311–314.

Cho, H., De Rooij, G.H., Inoue, M., Toride, N., 1999. Fingered flow: the role of the induction zone below the soil surface and the capillary fringe. Annual Meetings of the American Society of Agronomy, Crop Science Society of America, and Soil Science Society of America, Salt Lake City, UT, October 31–November 4, 1999.

Gardner, W.R., 1958. Some steady state solutions of unsaturated moisture flow equation with application to evaporation from a water table. Soil Sci. 85, 228–232.

van Genuchten, M.Th., 1980. A closed-form equation for predicting the hydraulic conductivity of unsaturated soils. Soil Sci. Soc. Am. J. 4, 892–898.

van Genuchten, M.Th., Nielsen, D.R., 1985. On describing and predicting the thermal and hydraulic properties of unsaturated soils. Ann. Geophys. 3, 268–315.

Gupta, S.C., Dowdy, R.H., Larson, W.E., 1977. Hydraulic and thermal properties of a sandy soil as influenced by incorporation of sewage sludge. Soil Sci. Soc. Am. J. 41, 601–605.

Haridasan, M., Jensen, R.D., 1972. On the calculation of hydraulic conductivity. Soil Sci. Soc. Am. Proc. 27, 263–265.

Khaleel, R., Relyea, J.F., 2001. Variability of Garnder's α for coarse textured sediments. Water Resour. Res. 37 (6), 1567–1575.

Klute, A., Scott, E.J., Whisler, F.D., 1965. Steady state water flow in a saturated inclined slab. Water Resour. Res. 1 (2), 287–294.

Kung, K.-J.S., 1990a. Preferential flow in sandy vadose zone. I. Field observation. Geoderma 46, 51–58.

Kung, K.-J.S., 1990b. Preferential flow in sandy vadose zone. II. Mechanism and implications. Geoderma 46, 59–71.

Kung, K.-J.S., 1993. Laboratory observation of the funnel flow mechanism and its influence on solute transport. J. Environ. Qual. 22, 91–102.

Liu, Y., Steenhuis, T.S., Parlange, J.-Y., 1994. Formation and persistence of fingered flow fields in coarse grained soils under different moisture contents. J. Hydrol. 159, 187–195.

Miyazaki, T., 1988. Water flow in unsaturated soil in layered slopes. J. Hydrol. 102, 201–214.

Morris, C.E., Stormont, J.C., 1997. Capillary barriers and subtitle D covers: estimating equivalency. J. Environ. Engng 123 (1), 3–10.

Rasmuson, A., Erikson, J.C., 1988. On the physico-chemical basis for the capillary barrier effect. Nordic Hydrol. 19, 281–292.

Ritsema, C.J., Steenhuis, T.S., Parlange, J.-Y., Dekker, L.W., 1996. Predicted and observed finger diameters in field soils. Geoderma 70, 185–196.

Ross, B., 1990. The diversion capacity of capillary barriers. Water Resour. Res. 26 (10), 2625–2629.

Selker, J., 1997. Design of interface shape for protective capillary barriers. Water Resour. Res. 33 (1), 259–260.

Selker, J.S., Leclerq, P., Parlange, J.-Y., Steenhuis, T.S., 1992. Fingered flow in two dimensions. Part 1. Measurement of matric potential. Water Resour. Res. 28 (9), 2513–2521.

Sisson, J.B., vanGenuchten, M.Th., 1992. Estimation of hydraulic conductivity without computing fluxes. In: vanGenuchten, M.Th., Leij, F.J., Lund, L.J. (Eds.), Indirect Methods for Estimating the Hydraulic Properties of Unsaturated Soils, University of California, Riverside, CA, pp. 665–674.

Staple, W.J., 1969. Comparison of computed and measured moisture redistribution following infiltration. Soil Sci. Soc. Am. Proc. 33, 840–847.

Steenhuis, T.S., Kung, K.-J.S., Parlange, J.-Y., Selker, J.S., Chen, X., 1990. Flow regimes in sandy soils with inclined layers. In: H. Morel-Seytoux (Ed.), Proceedings of 10th Annual AGU-Hydrology Days, Colorado State University, Fort Collins, April 10–12, pp. 78–94.

Steenhuis, T.S., Parlange, J.-Y., Kung, K.-J.S., 1991. Comment on: 'the diversion capacity of capillary barriers' by Benjamin Ross. Water Resour. Res. 27 (8), 2155–2156.

Topp, G.C., 1969. Soil water hysteresis measured in a sandy loam and compared with the hysteresis model. Soil Sci. Soc. Am. Proc. 33, 645–651.

Vachaud, G., 1967. Determination of the hydraulic conductivity of unsaturated soils from an analysis of transient flow data. Water Resour. Res. 3, 697–705.

Veneman, P.L.M., 1974. Measurements of soil moisture retention characteristics. In: Bouma, J., Baker, F.G., Veneman, P.L.M. (Eds.), Measurement of Water Movement in Soil Pedons above the Water Table, Information Circular No. 27, University of Wisconsin, Madison, WI.

Walter, M.T., Kim, J.-S., Steenhuis, T.S., Parlange, J.-Y., Heilig, A., Braddock, R.D., Selker, J.S., Boll, J., 2000. Funneled flow mechanisms in a sloping layered soil: laboratory investigations. Water Resour. Res. 34 (4), 841–849.

Webb, S.W., 1997. Generalization of Ross tilted capillary barrier diversion formula for different two-phase characteristic curves. Water Resour. Res. 33 (8), 1855–1859.